JOURNAL OF CATALYSIS 28, 477-488 (1973)

Alumina as a Textural Promoter of Iron Synthetic Ammonia Catalysts

H. TOPSØE, J. A. DUMESIC, AND M. BOUDART

Stauffer Laboratories of Chemistry and Chemical Engineering, Stanford University, Stanford, California 94305

Received October 2, 1972

The location of the Al_2O_3 in a reduced singly promoted iron catalyst (3% Al_2O_3 with 250 Å iron particles) was determined by Mössbauer spectroscopy. A mildly reduced catalyst exhibits a paramagnetic phase which disappears upon further reduction. The hyperfine parameters of the reduced catalyst agree with those of pure α-Fe. These observations are best reconciled with the idea that the Al_2O_3 is present in the α-iron in the form of ca. 30 Å inclusions consisting of $FeAl_2O_4$ in the incompletely reduced catalyst and of Al_2O_3 itself after thorough reduction.

INTRODUCTION

The ammonia synthesis has traditionally been carried out using iron catalysts. It has also been common practice to add certain oxides (promoters) to the iron synthetic ammonia catalysts. Mixtures of iron oxides and appropriate promoter oxides are fused together at high temperature giving a spinel-type structure which is then reduced to the active catalyst.

Emmett and Brunauer (*1, 2*) showed that the addition of promoter oxides such as Al_2O_3, K_2O and Na_2O increases considerably the total surface area per gram of the reduced catalyst. In their pioneering work on the use of gas adsorption in determining total, iron, and promoter surface areas, these authors found that iron synthetic ammonia catalysts promoted with small amounts of oxides (ca. 1%) have up to 70% of their surface covered with promoter. In agreement with the idea that a substantial fraction of promoters is at the surface of the iron crystallites, Nielsen *et al.* (*3*) observed that the X-ray diffraction pattern of a promoted iron catalyst was identical to that of pure α-Fe. In addition, D_2 exchange (*4*) and $H_2{}^{18}O$ exchange (*5*) have been used to determine the fraction of the surface covered with promoter, and the results of these studies are very close to those reached in the original chemisorption studies.

On the other hand, Hosemann *et al.* have recently (*6–9*) investigated a singly promoted iron synthetic ammonia catalyst containing 3% Al_2O_3 (at. % based on α-Fe). From a detailed analysis of X-ray diffraction data, they reached a conclusion which is at variance with the preceding ideas about the location of the promoter in the reduced catalyst. Their results seem to indicate that the major portion of the aluminum is present inside the α-Fe lattice as randomly distributed $FeAl_2O_4$ groups. The observed diffraction lines were those arising from α-Fe, and the observed lattice constant was equal to that of pure iron in agreement with previous investigations (*3*). Broadening of these diffraction lines, however, was detected when the experimental line widths were compared to those of a perfect single crystal of α-Fe. This broadening was interpreted as being due to the small size of the crystallites (ca. 250 Å) and to slight lattice distortions describable as paracrystalline lattice defects. These defects were attributed to $FeAl_2O_4$ groups incorporated in a three dimensional manner throughout the α-Fe host lattice, with the

Copyright © 1973 by Academic Press, Inc.
All rights of reproduction in any form reserved.

Fe^{2+}-ion located at a Fe-lattice site and surrounded by four O^{2-}-ions in the form of a tetrahedron distorted in the z-direction. The Al^{3+}-ions were assigned positions on the z-axis above and below the tetrahedron. All told, the $FeAl_2O_4$ molecule would replace seven α-Fe lattice sites. Such an arrangement, it was argued, would not change the average lattice constant from that of pure α-Fe. By annealing the catalyst, the authors concluded that the broadening of the diffraction lines was due to paracrystalline lattice defects and not to strain.

Recently Solbakken, Solbakken, and Emmett (*5*) have used $H_2{}^{18}O$ exchange to show that alumina molecules at the surface are present as a single layer. From this result it follows that for a singly promoted iron synthetic ammonia catalyst (3% Al_2O_3) with a particle size of about 250 Å, a large portion of the aluminum may be present inside the iron particles. The exchange experiments with $H_2{}^{18}O$, however, give no information about the state of the aluminum inside the iron crystallites.

Traditionally, the effect of the aluminum as a textural promoter, which prevents sintering, has been linked with the assumption that the aluminum is located mostly on the surface. With Hosemann's observation that a substantial fraction of the aluminum should be present inside the iron particles, however, the role of the promoter must be examined in greater detail.

Previous Mössbauer experiments obtained at Stanford (*10*) also reported by Hosemann in (*9*) showed no significant difference in the hyperfine parameters of a catalyst containing 1.16% Al_2O_3 and those of pure α-Fe. This lead us to conclude that random $FeAl_2O_4$ groups could not be present. Hosemann (*9*) suggests that clusters of about 10 $FeAl_2O_4$ molecules could be present inside the α-Fe and be consistent with his X-ray diffraction results and our Mössbauer investigations.

In order to obtain additional information about the state of the aluminum inside the iron particles (i.e., whether the aluminum is present as $FeAl_2O_4$ molecules as proposed by Hosemann *et al.*), a more detailed Mössbauer study was undertaken on the catalyst which Hosemann used in his investigation. We are indebted to Professor Dr. R. Hosemann for kindly providing us a sample of this catalyst.

EXPERIMENTAL

Mössbauer Spectrometer

The spectrometer is described in detail elsewhere (*11*, *12*), but the important features of the apparatus are described below. A 100 mc $^{57}Co/Cu$ source kept at room temperature was mounted on an Austin Science Associates drive unit, while the γ-ray detection was carried out using a Kr–CO_2 filled proportional counter tube (RG-61). A ND2200 512 channel multichannel analyzer was used for storage of the γ-ray counts. The spectrometer was operated in the constant acceleration Flyback mode (*11*) which enables full use of all 512 channels for storage of one spectrum. Absolute velocities were determined for each channel of the multichannel analyzer by means of an Austin Science Associates helium laser interferometer calibration system (*13*). This greatly enhances the accuracy of the spectrum since the laser calibration is done simultaneously with γ-ray counting. Positive velocity corresponds to the source moving towards the absorber. In order to make estimates of absolute areas and to compare areas from different spectra, corrections for the nonresonant background count rate were made according to the procedure described by Housley *et al.* (*14*).

The standard deviation in the number of counts collected is equal to the reciprocal square root of the number of counts. In the present study detectability of minute changes in the Mössbauer spectra was important, and in all the spectra reported here, more than 1.4 million counts in each of the 512 channels were collected giving a relative error of each data point less than 0.08%.

The multichannel analyzer output, which contains laser and γ-ray counts, is analyzed by a digital computer. The laser data are least-square fitted to give the absolute velocities used in the computer fit of the γ-ray data. This computer program utilizes a version of the Argonne variable metric minimization program to fit Lorentzian line shapes and can be used with or without linear constraints (*12*). The parabolic curvature of the background, due to the variable source–detector distance, is also accounted for in the computer fit.

Sample Preparation and Reduction

The singly promoted catalyst which had been reduced at 400°C in a $H_2:N_2$ mixture by Hosemann was received by us in the reduced state. The sample was ground in a mortar and 0.0345 g of the catalyst was mixed with 0.2151 g of 48 mesh Graphon (Cabot Corporation) which was found to be a convenient diluent in the preparation of samples. This mixture was compressed into a ¾ in. diameter wafer using a Carver press and was loaded into a stainless-steel water-jacketed vacuum cell designed for heating to temperatures of 500°C. The cell transmission windows were made of 10-mil thick beryllium discs (Kawecki Berylco Inc.) which contained less than 50 ppm iron. In order to control the gaseous atmosphere over the sample, the cell was connected to a multipurpose gas handling-vacuum system which allowed the evacuation to pressures of about 10^{-6} Torr and the flowing of H_2 gas at atmospheric pressure. The H_2 gas was purified in this system by passing the gas through a Deoxo catalytic hydrogen purifier (Engelhard), and then removing the water formed in a liquid nitrogen trap.

The reduction process was studied by recording Mössbauer spectra after various hydrogen treatments. The wafer was first heated in flowing hydrogen at 300°C for ½ hr. Mössbauer spectra were then taken at velocity ranges of ±3 mm/s and ±10 mm/s at 10^{-5} Torr and room temperature (24 ± 1°C). Following this treatment, the sample was heated to 415°C in flowing hydrogen for 25 min, and Mössbauer spectra were taken at 10^{-5} Torr and room temperature. A final reduction was performed by heating the sample to 425°C for 23 hr in flowing hydrogen, and the Mössbauer spectra were again taken at 10^{-5} Torr, room temperature, and velocity ranges of ±3 mm/s and ±10 mm/s.

The above evacuations were carried out in order to remove water from the cell. Since the beryllium discs and the cell walls were cooled during the reductions, the water formed during the reduction may well have been condensed inside the cell. If kinetic measurements were to be taken with the sample, this evacuation procedure would probably have introduced enough contamination to make the kinetic results meaningless. However, slight contamination of the surface will not affect the Mössbauer results, because the dispersion of the sample

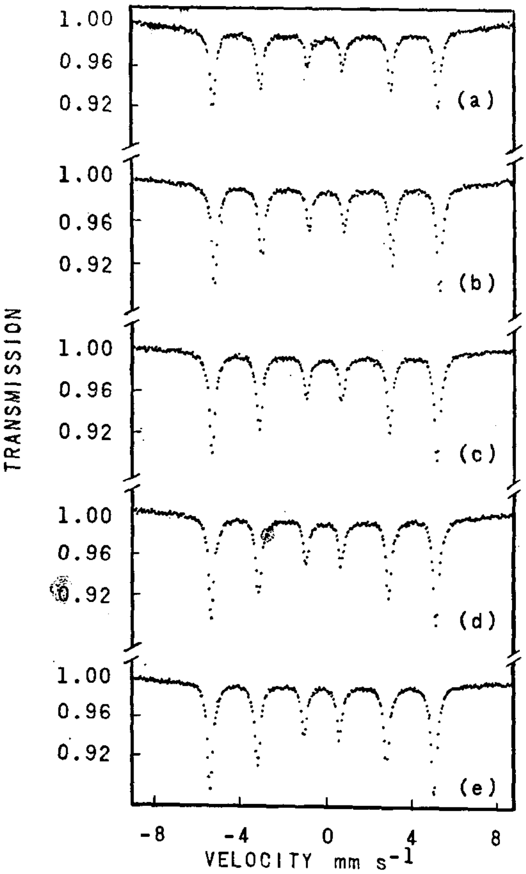

FIG. 1. Room temperature Mössbauer spectra at ±10 mm/s velocity range. (a) 3% Al_2O_3/Fe unreduced, (b) 3% Al_2O_3/Fe reduced in H_2 at 300°C for ½ hr, (c) 3% Al_2O_3/Fe reduced in H_2 at 415°C for 25 min, (d) 3% Al_2O_3/Fe reduced in H_2 at 425°C for 23 hr, (e) 1-mil Fe NBS foil.

is quite small. In addition, the probable presence of traces of N_2 in the H_2 used for reduction will tend to minimize the effect of other contaminants due to the strong chemisorption of N_2. Indeed, the best evidence that contamination of the sample is not important in this study is that pure α-Fe is detected in the Mössbauer spectrum after the long reduction at 425°C.

Results

In Figs. 1 and 2 are shown the Mössbauer spectra of the catalyst after successive reductions, the reductions becoming progressively more severe. After each reduction step, two Mössbauer spectra were taken, one at ±10 mm/s velocity range (Fig. 1) to scan the magnetically split portion of the spectrum and one at ±3 mm/s velocity range (Fig. 2) to obtain improved resolution of that region of the spectrum where paramagnetic peaks may occur. Figure 1 also shows the spectrum of a 1-mil Fe foil standard obtained from the National Bureau of Standards.

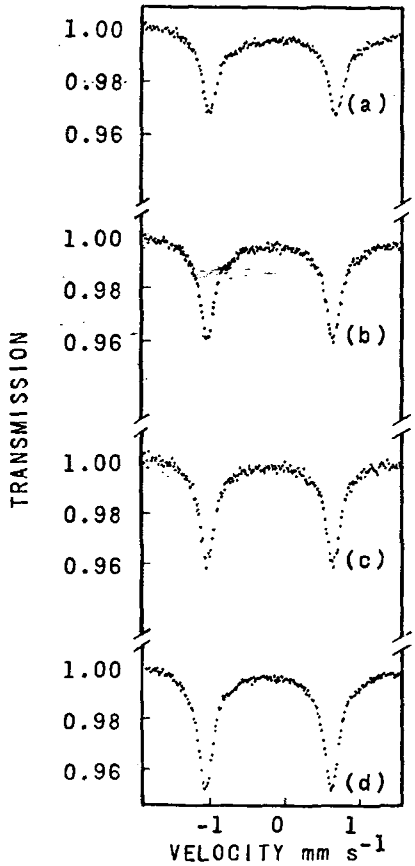

Fig. 2. Room temperature Mössbauer spectra at ±3 mm/s velocity range. (a) 3% Al_2O_3/Fe unreduced, (b) 3% Al_2O_3/Fe reduced in H_2 at 300°C for ½ hr, (c) 3% Al_2O_3/Fe reduced in H_2 at 415°C for 25 min, (d) 3% Al_2O_3/Fe reduced in H_2 at 425°C for 23 hr.

The Mössbauer spectral parameters are given in Tables 1 and 2 for the ±10 mm/s and ±3 mm/s spectra, respectively. The hyperfine fields were determined (*11*) from the splitting between peak 1 and peak 6 [$(v_6 - v_1)$ in mm/s] using the relation that the field, H, (in kOe) is equal to $31.090 \times (v_6 - v_1)$. The quadrupole interaction, was determined from the relation $\epsilon = (v_6 - v_5 - v_2 + v_1)/4$. Isomer shifts with respect to the ^{57}Co/Cu source, δ_{Cu}, (in mm/s) were calculated using the formula, $\delta_{\mathrm{Cu}} = (v_6 + v_5 + v_2 + v_1)/4$. Γ_i is the linewidth (full-width at half-maximum) of peak i.

Figure 2 shows that each peak has a barely observable shoulder on the positive velocity side. It must be made clear that this is not a characteristic of the catalyst but is attributable to instrumental effects, since similar shoulders were observed on the spectrum of a sodium nitroprusside standard run on this spectrometer.

It might also be thought that the linewidths in Fig. 1 are unusually broad for those of pure α-Fe. However, instrumental broadening of the spectral lines is dependent on the velocity range scanned. It is quite large in the ±10 mm/s velocity range ($\Gamma_3 \cong 0.33$ mm/s), whereas the broadening at the ±3 mm/s velocity range is negligible ($\Gamma_3 \cong 0.25$ mm/s) when the thickness of the sample is taken into account (2.87×10^{18} ^{57}Fe atoms/cm^2).

Figure 3 shows the background for the series of Mössbauer spectra taken at ±3 mm/s. In Tables 1 and 2 are shown the values of the background-corrected total spectral areas, A_T, where

$$A_T = \frac{\pi}{2} \times \sum_{i=1}^{N} (\text{fractional dip})_i \times \Gamma_i \times B.$$

TABLE 1

MÖSSBAUER DATA FOR ±10 MM s^{-1} SPECTRA

	3% Al_2O_3/Fe passivated in air	3% Al_2O_3/Fe reduced in H_2 300°C, $\frac{1}{2}$ hr	3% Al_2O_3/Fe reduced in H_2 415°C, 25 min	3% Al_2O_3/Fe reduced in H_2 425°C, 23 hr	1 mil Fe NBS Foil
H, kOe	330.67 ± 0.06	330.61 ± 0.06	330.78 ± 0.06	330.63 ± 0.06	330.59 ± 0.05
ϵ, mm s^{-1}	−0.0066 ± 0.0011	−0.0049 ± 0.0011	−0.0050 ± 0.0011	−0.0046 ± 0.0011	−0.0050 ± 0.0010
δ_{Cu}, mm s^{-1}	−0.2218 ± 0.0011	−0.2206 ± 0.0011	−0.2196 ± 0.0011	−0.2198 ± 0.0011	−0.2197 ± 0.0010
Γ_6, mm s^{-1}	0.3170 ± 0.0029	0.3153 ± 0.0027	0.3156 ± 0.0029	0.3194 ± 0.0029	0.3415 ± 0.0026
Γ_3, mm s^{-1}	0.2933 ± 0.0080	0.3093 ± 0.0059	0.3312 ± 0.0078	0.3022 ± 0.0067	0.3020 ± 0.0043
A_T, see text	0.1476 ± 0.0060	0.1949 ± 0.0038	0.2095 ± 0.0052	0.2123 ± 0.0046	0.5725 ± 0.0069

TABLE 2
Mössbauer Data for ±3 mm s^{-1} Spectra

	3% Al_2O_3/Fe passivated in air	3% Al_2O_3/Fe reduced in H_2 300°C, ½ hr	3% Al_2O_3/Fe reduced in H_2 415°C, 25 min	3% Al_2O_3/Fe reduced in H_2 425°C, 23 hr
Γ_3, mm s^{-1}	0.2531 ± 0.0040	0.2570 ± 0.0033	0.2540 ± 0.0039	0.2528 ± 0.0020
A_3, see text	0.0119 ± 0.0004	0.0166 ± 0.0003	0.0173 ± 0.0004	0.0178 ± 0.0002
A_4, see text	0.0116 ± 0.0004	0.0159 ± 0.0003	0.0163 ± 0.0004	0.0176 ± 0.0002
A_T, see text	0.1414 ± 0.0060	0.1948 ± 0.0042	0.2017 ± 0.0051	0.2124 ± 0.0028

The background correction factor, B, takes into account the fact that radiation besides the 14.4 keV γ-ray was detected, and B was constant within 1% throughout the experiments. The values of A_T in Table 1 are calculated by summing over i from 1 to 6, while the values of A_T in Table 2 are found by summing over i from 3 to 4 and multiplying this value by 6, i.e., a 3:2:1:1:2:3 intensity ratio of the 6-line spectrum was assumed.

Error estimates of the parameters listed in Tables 1 and 2 were obtained from the standard deviations calculated by the computer program. The main error in the parameters such as the magnetic fields may indeed be due to the slight variation of ambient temperature since $\Delta H/\Delta T \cong 0.36$ kOe/K (*15*). Independent X-ray line broadening studies at Stanford verified the particle size of 200–250 Å, as reported by Hosemann *et al.* (*6*).

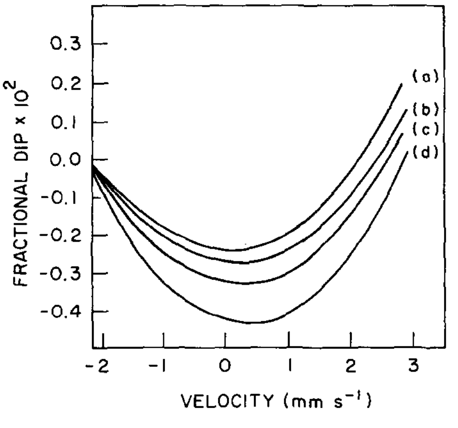

Fig. 3. Background curves for room temperature Mössbauer spectra at ±3 mm/s velocity range. (a) 3% Al_2O_3/Fe reduced in H_2 at 425°C for 23 hr, (b) 3% Al_2O_3/Fe reduced in H_2 at 415°C for 25 min, (c) 3% Al_2O_3/Fe reduced in H_2 at 300°C for ½ hr, (d) 3% Al_2O_3/Fe unreduced.

Discussion

Surface Oxidation and Its Detection by Mössbauer Spectroscopy

Figure 1 shows the Mössbauer spectra of the catalyst after exposure to air and after successive reductions. The spectrum of the catalyst which has been exposed to air does not show the presence of any new phase, which at first may appear somewhat puzzling since it is known that iron catalysts skin oxidize to a depth of several layers at room temperature. After the reduction at 425°C the spectrum does not appear to have changed appreciably. Furthermore, the hyperfine parameters (see Table 1) of the 6-line spectrum of the oxidized catalyst are equal to those of the standard iron foil within experimental error.

In our present sample we can, however, determine how much of the iron has been oxidized at room temperature, even without detecting the appearance of a separate spectral component arising from the oxidized iron. This is done by comparing the background-corrected areas of the α-Fe spectrum before reduction and after the 415°C reduction; the result is a 25% increase in the area upon reduction.

Thus the oxidized form of iron does not show a separate well-defined Mössbauer spectrum but rather gives rise to a broad component which is not detectable (without a detailed analysis).

With an average particle size of 250 Å

and the surface half covered with promoter we can estimate, assuming that only the bare portion of the iron surface is oxidized, that the oxide layer has a thickness of about 20 Å. This is in agreement with other oxidation results in the presence of water vapor (*16*). The composition of these oxide films has been found (*16*) to vary in stoichiometry and would not, therefore, be expected to give rise to a sharp Mössbauer spectrum. A careful analysis, described in detail later, of the background curvature enables us to detect the presence of broadened Mössbauer components. This analysis (see Fig. 3) shows the disappearance of a broad spectral component upon reduction of the catalyst, the area of which is in good agreement with the simultaneously observed increase in the hyperfine area mentioned above.

From the above it should be noted that nonstoichiometric phases in small amounts cannot be detected by a superficial treatment of the Mössbauer spectra but can be found by a more careful analysis.

Magnetically Hyperfine Split Spectra

The proposal by Hosemann that the aluminum is present inside the iron particles as randomly distributed $FeAl_2O_4$ molecules must be checked with respect to consistency with Mössbauer data. The presence of these molecules should have two major effects on the Mössbauer spectra. First, it is expected that the hyperfine parameters of the catalyst should be different from those of pure iron, and second, the presence of a Fe^{2+} component should be observed. The effect on the hyperfine spectrum will be discussed first.

Molecules of $FeAl_2O_4$, if present, would distort the symmetry of the neighboring iron atoms resulting in larger quadrupole interactions than those in pure iron. Even small changes in the quadrupole splitting can be detected by measuring the broadening of the α-Fe spectral lines. The magnetic field at the iron nuclei will also be affected by the presence of these $FeAl_2O_4$ molecules as neighbors. It seems likely, to a first approximation at least, that the $FeAl_2O_4$ molecules will act as holes in the magnetic structure, in analogy to the role of aluminum or silicon in dilute iron alloys containing these elements. The magnetic field of iron in these alloys depends strongly on the number of noniron neighbors. Indeed, in these alloys (*17–19*) changes in the magnetic field at an iron nucleus were detected by the presence of noniron atoms as far away as the fifth neighbor shell. For the catalyst used in this study, it can be shown that approximately 50% of the iron atoms would have noniron atoms within their first three neighbor shells if the $FeAl_2O_4$ molecules were randomly distributed. This demonstrates the sensitivity of Mössbauer spectroscopy for the detection of these $FeAl_2O_4$ molecules. To be semiquantitative, the effect of $FeAl_2O_4$ groups in iron will be modeled by a dilute Fe–Al alloy.

The internal magnetic field at a given iron atom in the Fe–Al alloy depends strongly on the number of aluminum neighbors. The change in the magnetic field relative to that of pure α-Fe for any given site, ΔH, can be expressed as:

$$\Delta H = \sum_{n=1}^{5} M_n \Delta H_n$$

where M_n is the number of solute atoms in the nth neighbor shell and ΔH_n is the internal field shift due to solute atoms in the nth shell. It is apparent that the alloying of Al into the α-Fe lattice will create a distribution of fields, thus producing broad spectral lines with non-Lorentzian shapes. In addition, the isomer shift of the iron increases regularly with an increase in the number of aluminum neighbors.

The hyperfine parameters of the Mössbauer spectra for the singly promoted catalyst and the NBS iron standard are listed in Table 1. The value of the hyperfine field of the catalyst does not vary, within experimental error, for different degrees of reduction and is equal, within experimental error, to that of the iron standard.

For dilute Fe–Al alloys (*18*) the change in the magnetic field with respect to the aluminum concentration is about 2 kOe/

at. %. The results of this study, therefore, indicate that less than 2% of the aluminum in the catalyst could be present as randomly distributed $FeAl_2O_4$ molecules, assuming that one $FeAl_2O_4$ molecule acts as one aluminum hole. Because a $FeAl_2O_4$ molecule surely behaves like more than one hole, the maximum amount of aluminum present as $FeAl_2O_4$ molecules is less than the above limit of 2%. Thus, Hosemann's original proposal of randomly distributed $FeAl_2O_4$ molecules must be discarded.

The results of a preliminary Mössbauer investigation (*10*) conducted in this laboratory on a catalyst containing 1.16% Al_2O_3 also showed pure α-Fe behavior. Hosemann (*9*) explained these results by the presence of clusters of about 10 $FeAl_2O_4$ molecules. From the present results it appears that clusters of about 100 $FeAl_2O_4$ molecules would be necessary in order that the magnetic field would not be perturbed, if $FeAl_2O_4$ is indeed present.

The Mössbauer spectra also exclude the possibility of an Fe–Al alloy with an aluminum content greater than 0.03%. Also from X-ray investigations reviewed by Nielsen *et al.* (*3*) the lattice constant of the α-Fe phase of a singly promoted catalyst was identical within experimental error to that of pure α-Fe. The experimental errors in these X-ray diffraction experiments put an upper limit of 0.3% on the amount of aluminum as an alloying element. The results obtained by Mössbauer spectroscopy and X-ray diffraction are in good agreement with each other although it must be noted that the former method is 10 times more sensitive than the latter to small amounts of aluminum in α-Fe.

That very pure iron is present is also shown by the equality of the values of the isomer shift, quadrupole splitting, and linewidths between the singly promoted catalyst and the pure iron standard. The linewidths (Table 1) of the iron foil are actually larger than those of the catalyst. This is due to the fact that the number density of ^{57}Fe atoms is larger for a 1-mil foil than for the catalyst. When the linewidth (Γ_6) of the iron standard is corrected to the same number density as the catalyst, a value for Γ_6 of 0.3180 mm/s is obtained, in agreement with the value of Γ_6 of the catalyst.

Paramagnetic Spectral Component

The effect of $FeAl_2O_4$ on the hyperfine splitting of the α-Fe Mössbauer spectrum has by now been dealt with; next, the detectability of $FeAl_2O_4$ from Mössbauer lines due to Fe^{2+} will be discussed.

The resulting Mössbauer spectrum might have some of the characteristics of the bulk $FeAl_2O_4$ spectrum. Bulk $FeAl_2O_4$ has a Néel temperature of about 8 K, thus under the experimental conditions of this study it will exhibit paramagnetic behavior. Several Mössbauer investigations (*20–22*) have been carried out on bulk samples of $FeAl_2O_4$, but these studies differ somewhat in the number of peaks observed. This discrepancy, however, seems most likely to be due to the different heat treatments used in the various investigations, resulting in different degrees of inversion of the spinel formed. Yagnik and Mathur (*22*) give the following values for the isomer shift and quadrupole splitting, QS, of the tetrahedrally located Fe^{2+} (A site) and the octahedrally located Fe^{2+} (B site), for a degree of inversion, x, equal to 0.23

Fe^{2+} in A site $\delta_{Cu} = 0.78$ mm/s QS = 1.39 mm/s
Fe^{2+} in B site $\delta_{Cu} = 1.20$ mm/s QS = 2.76 mm/s

Thus, peaks would be expected to be present at 0, 1.48, and 2.58 mm/s with respect to our source if a partially inverse $FeAl_2O_4$ structure is present. Alternatively, if a truly normal structure is present, a quadrupole splitting will not be observed since the perfect cubic symmetry around the tetrahedral Fe^{2+}-ion will not produce an electric field gradient. A single peak at about 0.7 mm/s with respect to our source should, therefore, be observed if the above symmetry is present.

The positions of the third, fourth, and fifth iron peaks are −1.06, 0.60, and 2.85 mm/s, respectively. From these peak positions it can be seen that the iron spectrum will not interfere with the detection of a partially inverse $FeAl_2O_4$ structure. From the spectra shown in Fig. 2 it is apparent that no additional peaks due to a partially inverse $FeAl_2O_4$ structure are present.

If the $FeAl_2O_4$ is present as a completely normal spinel, then the area of peak 4 in the iron spectrum would be greater than that of peak 3 because of an additional paramagnetic peak at a position of about 0.7 mm/s. From Table 2 it can be seen that this is not the case. Thus it can be concluded that a separate bulk phase of $FeAl_2O_4$ was not detected by the Mössbauer spectrometer. The maximum amount of bulk $FeAl_2O_4$ which could be present as a partly inverse or normal spinel and yet be undetectable was estimated to be about 0.2% of the total iron present. From this it follows that less than 15% of the aluminum is present in a form which has the characteristics of bulk $FeAl_2O_4$.

However, the absence of a characteristic bulk $FeAl_2O_4$ spectrum does not preclude the possible existence of $FeAl_2O_4$ clusters having a size of at least 30 Å, which is the minimum size consistent with the results of the hyperfine field analysis. The spectrum arising from these clusters would be expected to be broadened due to variation in quadrupole interactions resulting from very small particle size.

With this in mind, a careful analysis was made of the background curvature obtained from the computer fit after the different reduction steps. It was thought as mentioned earlier that this was the best method of analyzing for the possible presence of a very broad spectrum, and the results of this analysis are shown in Fig. 3. The main origin of the background curvature, as stated before, is the variable source–detector distance which occurs during the constant acceleration velocity sweep. Since this driving motion is the same for spectra with the same velocity range, changes in the background curvature from one spectrum to another give valuable information about the appearance or disappearance of peaks in the velocity region scanned.

From Fig. 3 it can be seen that increasing the degree of reduction results in the disappearance of a peak in the central region of the iron spectrum. From the shift in the minimum of the curves, it is concluded that this disappearing peak is located at about 0.5 mm/s.

At the end of the long reduction no paramagnetic phase is present since the background (corrected for the influence of all peaks) after this reduction has the same shape as the true background as determined by taking a spectrum when no sample was present in the cell, all other experimental conditions being kept the same. Also, at the end of the long reduction, the background minimum is located, within experimental error, at zero velocity, the point at which the source–detector distance is greatest.

It can be concluded that after reduction conditions more severe than that used by Hosemann, much less Fe^{2+} is present than the amount required if the Al is present as $FeAl_2O_4$, and the aluminum phase occluded from the surface is therefore most likely Al_2O_3.

On the other hand the state of the catalyst after the second reduction step at 415°C may indeed resemble that studied by Hosemann if it is agreed that the surface oxide has been sufficiently removed by the first two reductions. Therefore, any changes in the background and spectral areas upon further reduction must be caused by the disappearance of a phase, other than a surface oxide, giving rise to a broad spectrum.

The area change in the background between −1.3 and +2.7 mm/s (corresponding to $\delta_{Cu} = 0.7$ and QS = 4 mm/s) caused by the long reduction at 425°C is 1.14% of the total spectral area of the α-Fe. If indeed 3% (at. %) of the aluminum is present as $FeAl_2O_4$, then 1.5% of the iron must be present as Fe^{2+}. Since the recoil-free fraction of the Fe^{2+} in spinels (ca. 0.6) is somewhat lower than that of α-Fe (ca.

0.8), the number of Fe^{2+} ions responsible for the broad Mössbauer peak is, within experimental error, equal to 1.5% of the total number of Fe atoms as α-Fe. This is also consistent with the increase in the α-Fe spectral area of 1.3% upon the last reduction.

From these results one may argue that under the reduction conditions used by Hosemann, $FeAl_2O_4$ clusters may be present, but that these clusters disappear or are transformed into a phase not containing iron under more severe reductions. In many of the published laboratory investigations (*23–27*), the reductions are typically carried out for long times in pure hydrogen at temperatures in excess of 400°C. These conditions are closer to the pure hydrogen 23 hr reduction at 425°C used in this study than the 400°C reduction with a $H_2:N_2$ mixture used by Hosemann. Furthermore, the presence of N_2 in the reduction mixture used by Hosemann might decrease the severity of the reduction due to the chemisorption of nitrogen.

Hosemann mentioned that the observed broadening of the X-ray diffraction lines could be explained by the presence of ordinary strains in the α-Fe lattice but concluded that this was not the main cause of the broadening since this broadening of the lines persisted after annealing of the catalyst. This annealing will remove strain caused by dislocations and point defects, but it will not remove the strain caused by occluded Al_2O_3 or $FeAl_2O_4$ clusters in the α-Fe lattice. Hence, Hosemann's X-ray diffraction data could equally well be explained by the presence of Al_2O_3 inclusions in the α-Fe lattice. Thus, the reinterpreted X-ray data are also consistent with the conclusion of Solbakken *et al.* (*5*) that the aluminum on the surface is present as a single layer, i.e., a large fraction of the aluminum must be inside the iron particles, and also with the results of this investigation that Al_2O_3 inclusions are present inside the iron particles.

As mentioned previously, the effect of the alumina as a textural promoter has been traditionally associated with a surface phenomenon (*28*). It was known that singly promoted catalysts have a better resistivity toward sintering than pure iron catalysts and that the sintering of unpromoted iron particles occurs quite easily. Thus the layer of promoter on the surface was thought to form a barrier to the recrystallization process of iron particles and in this way function as a textural promoter.

The results of this study agree with those of others in that a large fraction of the aluminum is inside the iron particles. Besides, this work shows that the aluminum is present as an occluded phase that does not contain iron in a well reduced catalyst and is probably Al_2O_3. There is no *a priori* or experimental reason why aluminum promotion solely is caused by a single layer covering about 50% of the surface rather than by the major fraction of the aluminum which is inside of the iron particles. Therefore, the possible effect of this latter aluminum as a textural promoter must be considered. The existence of strain created by the occluded Al_2O_3 phase will shift the equilibrium particle size toward smaller particles since the ratio of strain to surface effects becomes greater for larger particles. Iron particles will grow until this equilibrium size is reached, and this size, which is smaller than the equilibrium size of pure iron particles, will be stabilized by the occluded Al_2O_3 (*29*).

With the above ideas in mind one could propose the following picture for the reduction process and the role of aluminum as a textural promoter. When the catalyst is in the unreduced state as Fe_3O_4, the aluminum is homogeneously distributed over the magnetite lattice as a solid solution between Fe_3O_4 and $FeAl_2O_4$ (*3*). This homogeneous distribution is represented in Fig. 4a. Due to the fact that $FeAl_2O_4$ is more difficult to reduce than Fe_3O_4 (*6*), the catalyst after the initial stages of reduction will tend to have aluminum-rich regions, as shown in Fig. 4b. After a certain degree of reduction, the aluminum-rich regions will still contain iron, as $FeAl_2O_4$ for example, but the remaining iron will have been reduced to very pure α-Fe. This situation is shown in Fig. 4c. It is likely that the reduction conditions used by Hosemann

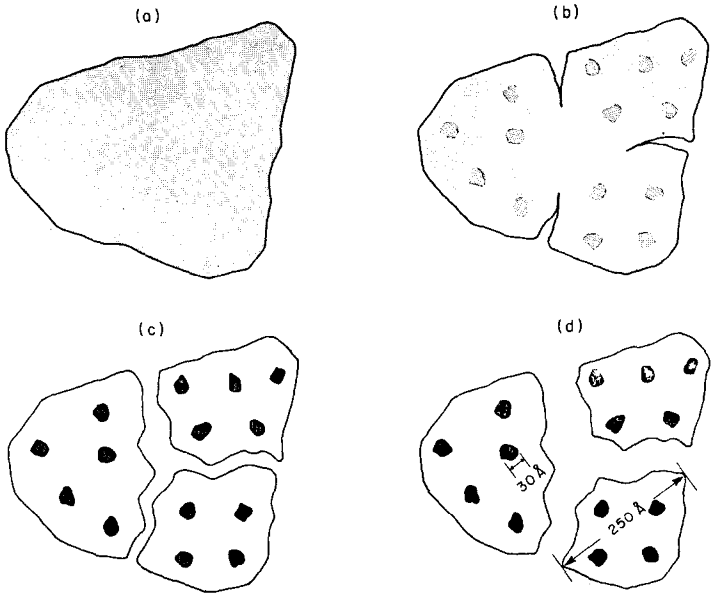

FIG. 4. Picture of the reduction process of the catalyst. (a) Unreduced large catalyst particle with the promoter distributed homogeneously. (b) Catalyst after short reduction. Aluminum-rich regions appear. (c) Catalyst after further reduction consists of α-Fe and $FeAl_2O_4$ inclusions. (d) Fully reduced catalyst. Consists of small α-Fe particles with Al_2O_3 inclusions.

have produced a catalyst with the above characteristics. Under more severe reduction conditions, however, the aluminum-rich regions do not contain iron, and the aluminum is probably present as Al_2O_3, as shown in Fig. 4d. These inclusions of Al_2O_3 create strain in the iron particles and could be partially responsible for the initial formation of small iron particles from the larger Fe_3O_4 particles during reduction. Subsequent stabilization of the iron particles might also be attributed to these Al_2O_3 inclusions. The observation that a promoted catalyst is more difficult to reduce than an unpromoted catalyst (*3*) is consistent with the above description of the reduction process. The promoting effect discussed above is theoretically reasonable, but further experimentation must be performed in order to ascertain its importance relative to that of the promoter located on the surface.

CONCLUSION

In this study it has been shown that the iron phase in a reduced singly promoted synthetic ammonia catalyst containing 3% Al_2O_3 is very pure α-Fe, and does not contain the randomly distributed $FeAl_2O_4$ molecules in the α-Fe lattice originally proposed by Hosemann *et al.* (*6*).

The results of Hosemann indicated strain in the α-Fe lattice, and the findings of Solbakken, Solbakken, and Emmett (*5*) showed that the promoter is not entirely at the surface. Although Hosemann's explanation of the origin of the strain is not consistent with the present Mössbauer investigation, our conclusion that an occluded phase consisting of large clusters is present may account for the strain observed by Hosemann.

ACKNOWLEDGMENTS

This work has been financed by the National Science Foundation (Grant GK 17451X). Fellowship support is gratefully acknowledged by JAD to the National Science Foundation. We are deeply indebted to J. M. Schultz for suggesting the promoter action mentioned in this paper, to R. L. Garten and K. A. Klinedinst for introductory Mössbauer work in this field, and to Professor R. Hosemann for providing us with the catalyst sample. We are also grateful to Professor P. H. Emmett for many stimulating comments. Finally we wish to thank C. Bartholomew, Professors R. Metzger, R. A. Huggins, and J. E. Benson for valuable discussions.

REFERENCES

1. EMMETT, P. H., AND BRUNAUER, S., *J. Amer. Chem. Soc.* **59**, 1553 (1937).
2. EMMETT, P. H., AND BRUNAUER, S., *J. Amer. Chem. Soc.* **62**, 1732 (1940).
3. NIELSEN, A., MOLLER, C. K., AND RATHLEV, J., "An Investigation on Promoted Iron Catalysts for the Synthesis of Ammonia." 3rd ed., Chap. 7, 166, Jul. Gjellerups Forlag, Copenhagen, 1968.
4. SCHOLTEN, J. J. F., Thesis, Delft, The Netherlands (1959).
5. SOLBAKKEN, V., SOLBAKKEN, A., AND EMMETT, P. H., *J. Catal.* **15**, 90 (1969).
6. HOSEMANN, R., PREISINGER, A., AND VOGEL, W., *Ber. der Bunseng.* **70**, 796 (1966).
7. HOSEMANN, R., LEMM, K., SCHONFELD, A., AND WILKE, W., *Kolloid-Z. Z. Polym.* **216–217**, 103 (1967).
8. HOSEMANN, R., *Chem. Ing. Tech.* **42**, 1252 (1970).
9. HOSEMANN, R., *Chem. Ing. Tech.* **42**, 1325 (1970).
10. GARTEN, R. L., KLINEDINST, K. A., AND BOUDART, M., unpublished results, 1969.
11. TOPSØE, H., Ph.D. Dissertation, Stanford University, 1972.
12. BARTHOLOMEW, C., Ph.D. Dissertation, Stanford University, 1972.
13. COSGROVE, J. G., AND COLLINS, R. L., *Nucl. Instrum. Methods* **95**, 269 (1971).
14. HOUSLEY, R., ERICKSON, N. E., AND DASH, J. D., *Nucl. Instrum. Methods* **27**, 29 (1964).
15. PRESTON, R. S., HANNA, S. S., AND HEBERLE, J., *Phys. Rev.* **128**, 2207 (1962).
16. KRUGER, J., AND YOLKEN, H. T., *Corrosion* **20**, 29t (1964).
17. STEARNS, M. B., *J. Appl. Phys.* **35**, 1095 (1964).
18. JOHNSON, C. E., RIDOUT, M. S., AND CRANSHAW, T. E., *Proc. Phys. Soc.* **81**, 1079 (1963).
19. STEARNS, M. B., *Phys. Rev.* **147**, 439 (1966).
20. ROSSITER, M. J., *J. Phys. Chem. Solids* **26**, 775 (1965).
21. ONO, K., ITO, A., AND SYONO, Y., *Phys. Lett.* **19**, 620 (1965).
22. YAGNIK, C. M., AND MATHUR, H. B., *J. Phys. C.* **1** (ser. 2), 469 (1968).
23. SCHOLTEN, J. J. F., ZWILTERING, P., KPNVALINKA, J. A., AND DE BOER, J. H., *Trans. Faraday Soc.* **59**, 2166 (1959).
24. OZAKI, A., TAYLOR, H., AND BOUDART, M., *Proc. Roy. Soc. A* **258**, 47 (1960).
25. TANAKA, K., *J. Res. Inst. Catalysis* **13**(2), 119 (1965).
26. TAKEZAWA, N., AND TOYOSHIMA, I., *J. Res. Inst. Catal.* **14**(1), 41 (1966).
27. MORIKAWA, Y., AND OZAKI, A., Preprint from *J. Catal.* (1971).
28. NIELSEN, A., AND BOHLBRO, H., "An Investigation on Promoted Iron Catalysts for the Synthesis on Ammonia," 3rd ed., Chap. 9, p. 221, Jul. Gjellerups Forlag, Copenhagen, 1968.
29. SCHUTZ, J. M., *J. Catal.* **27**, 64 (1972).